Figure S1. Quality scores Illumina ("raw")

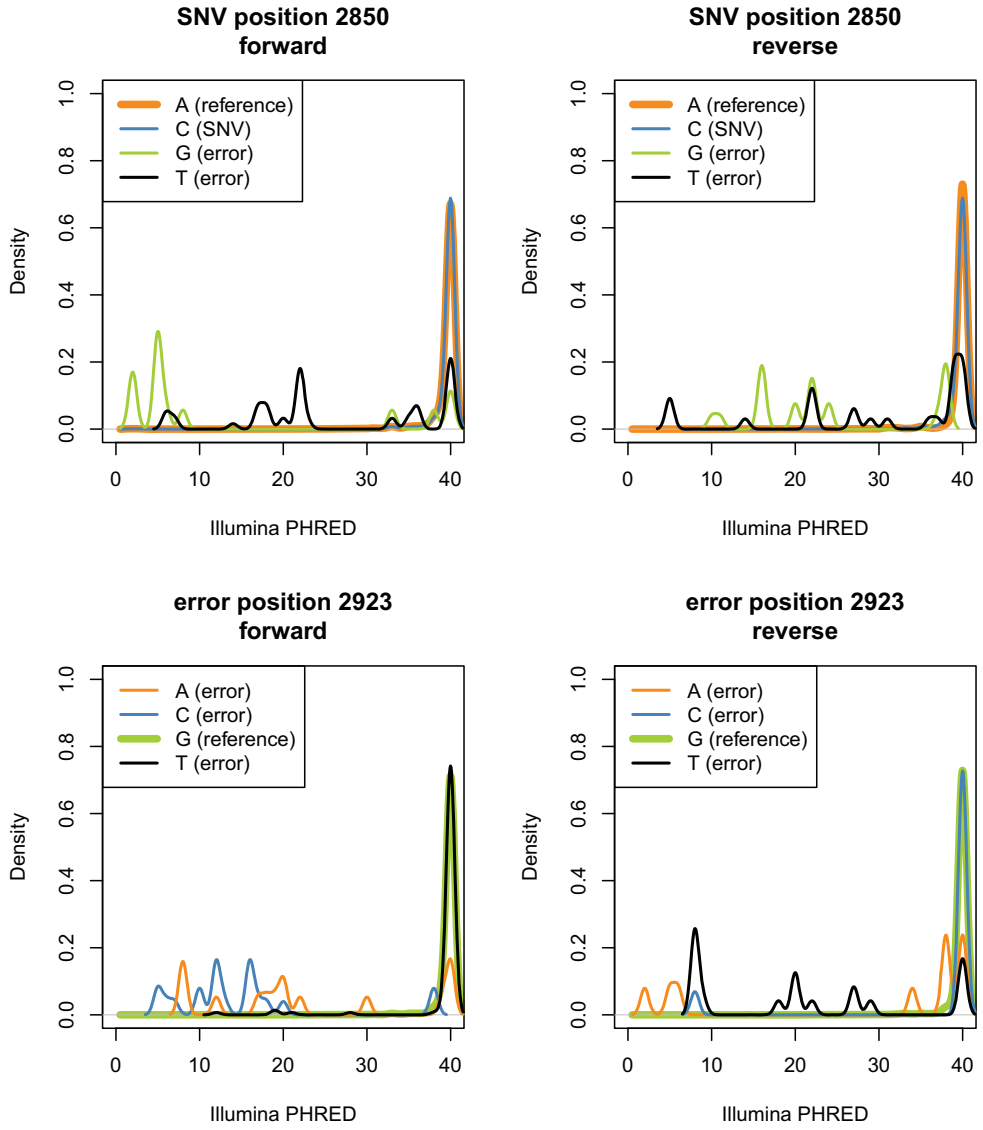

Distributional density of the Illumina PHRED scores per nucleotide (A/C/G/T) in the forward and reverse read mapping at SNV position 2850 and at error position 2923 for training sample 1 (out of 96 *in silico* read sets). The probability density distribution is different for errors compared to "no error" (reference/SNV) in forward and/or reverse read direction.

Figure S2. Quality Quantile plot ("raw")

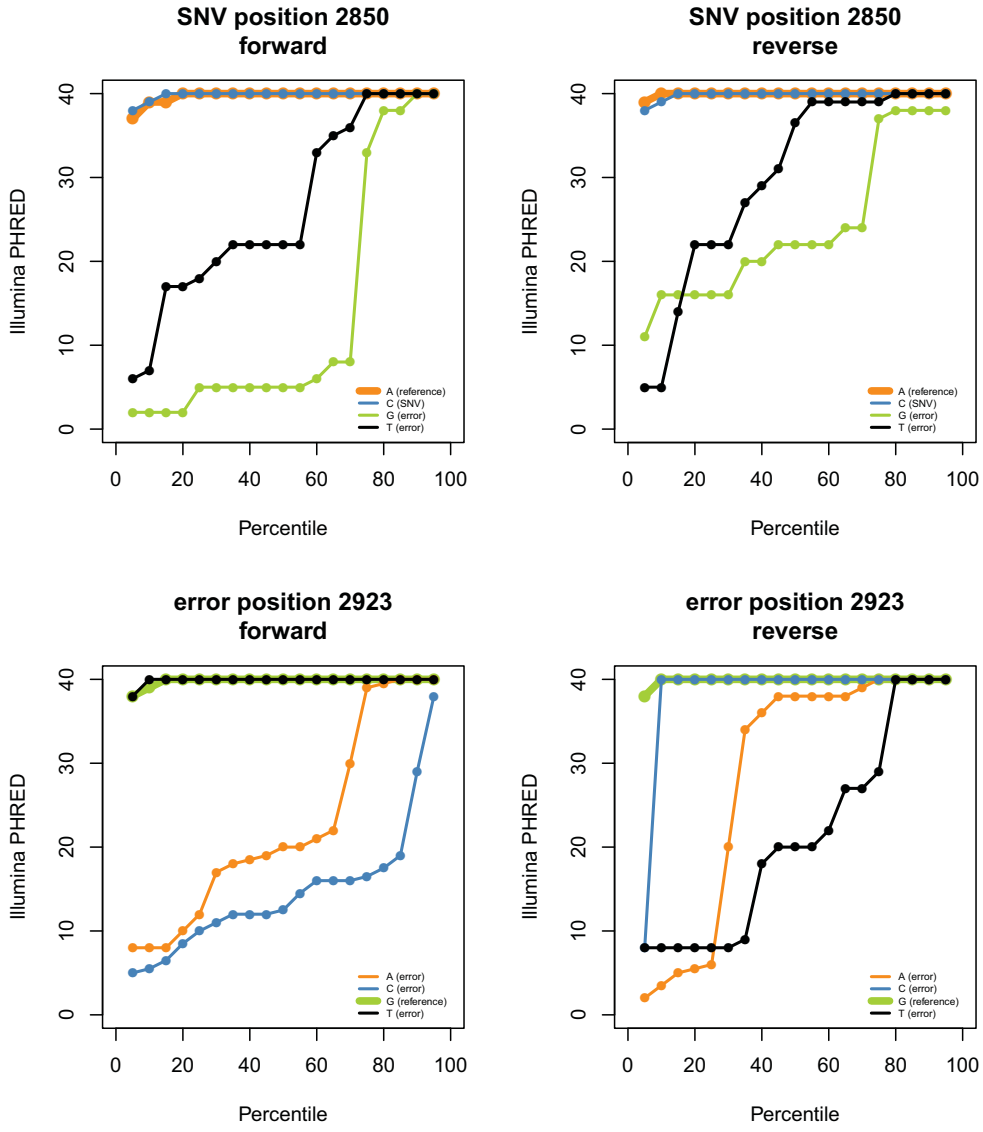

Illumina PHRED scores per nucleotide (A/C/G/T) in the forward and reverse read mapping summarized for nineteen percentiles (5^{th},10^{th},...,95^{th}) at SNV position 2850 and at error position 2923 for training sample 1 (out of 96 *in silico* read sets). The cumulative distribution is different for errors compared to "no error" (reference/SNV) in forward and/or reverse read direction.

Figure S3. Quality scores recalibrated

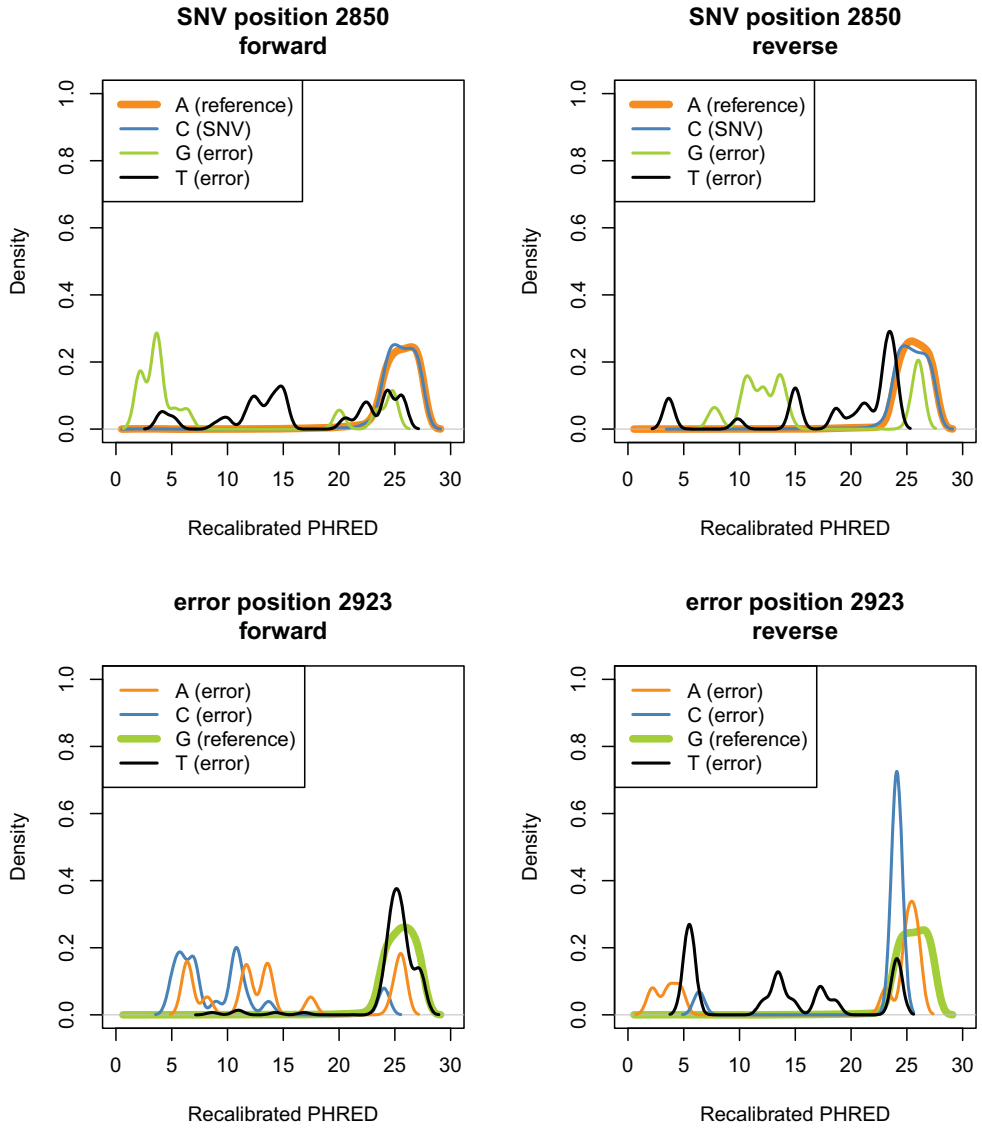

Distributional density of the recalibrated PHRED scores per nucleotide (A/C/G/T) in the forward and reverse read mapping at SNV position 2850 and at error position 2923 for training sample 1 (out of 96 *in silico* read sets). The probability density distribution is different for errors compared to "no error" (reference/SNV) in forward and reverse read direction.

Figure S4. Quality Quantile plot (recalibrated)

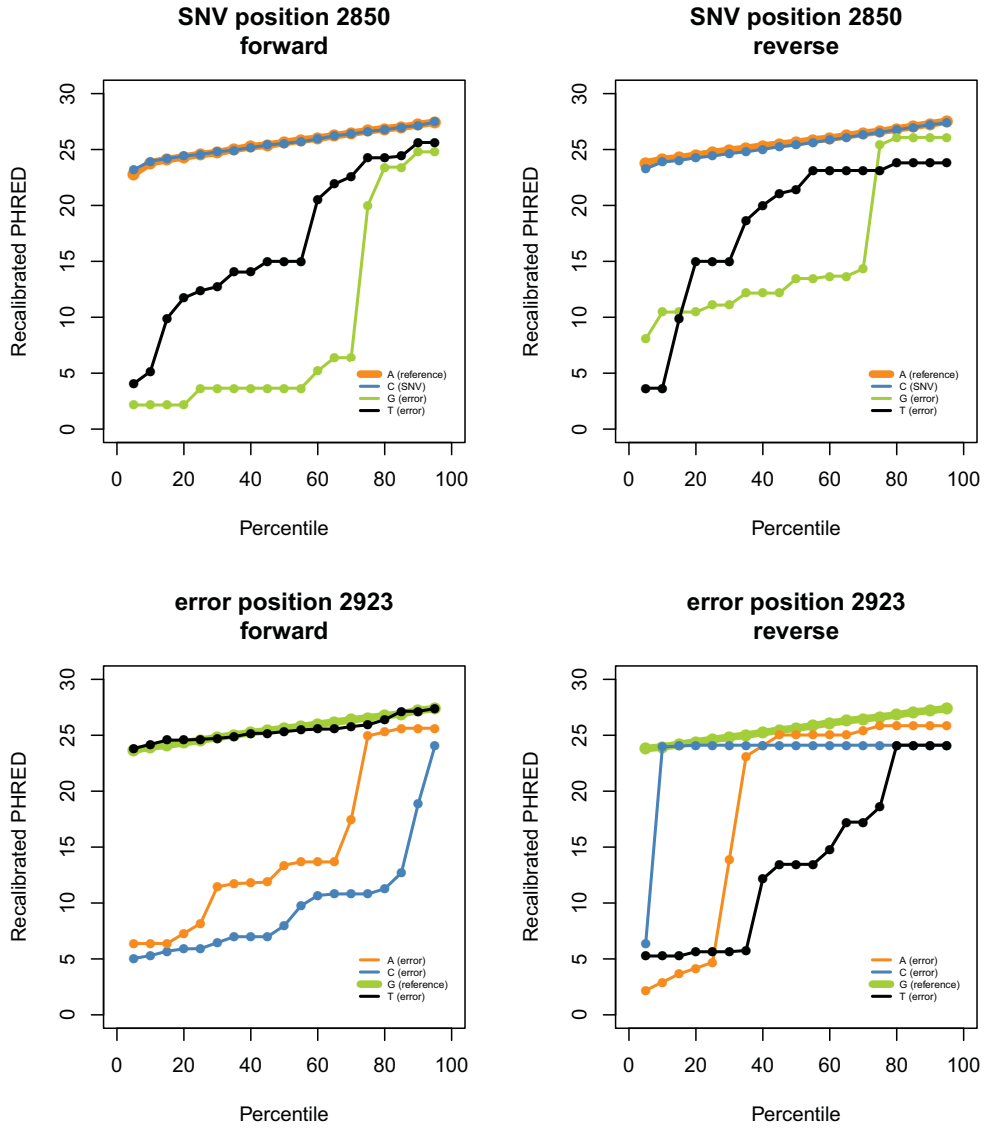

Recalibrated PHRED scores per nucleotide (A/C/G/T) in the forward and reverse read mapping summarized for nineteen percentiles (5^{th},10^{th},...,95^{th}) at SNV position 2850 and at error position 2923 for training sample 1 (out of 96 *in silico* read sets). The cumulative distribution is different for errors compared to "no error" (reference/SNV) in forward and reverse read direction.

Figure S5. Coverage of plasmids in FASTQ/1 training data

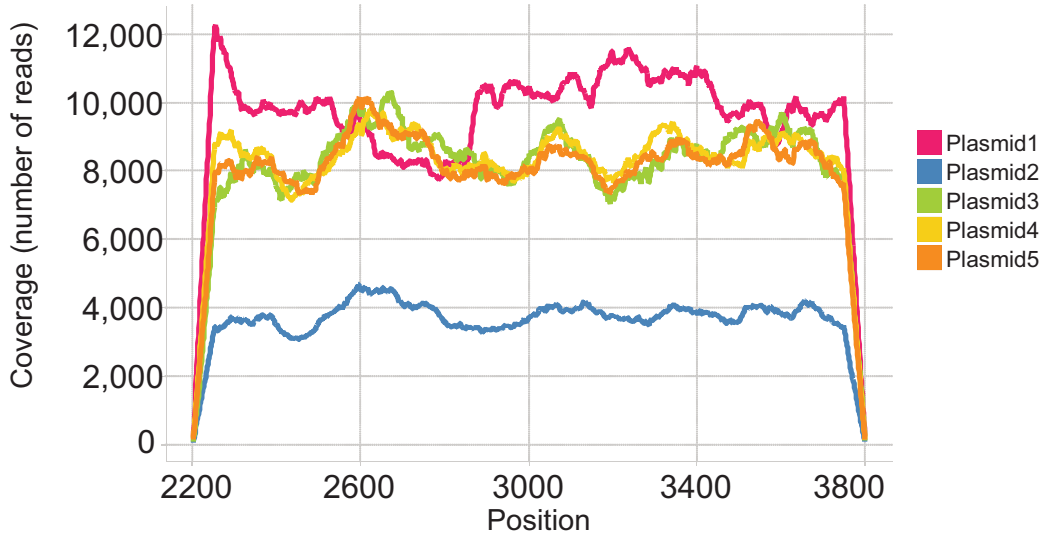

Five HIV−1 plasmids were sequenced with Illumina GAIIx in one lane. The coverage per plasmid derived from a total of 1,183,162 reads, with at least one nucleotide in the PR−RT region from nucleotide position 2253 to 3749, is shown.

Figure S6. SNVs in *in silico* set of 960 samples

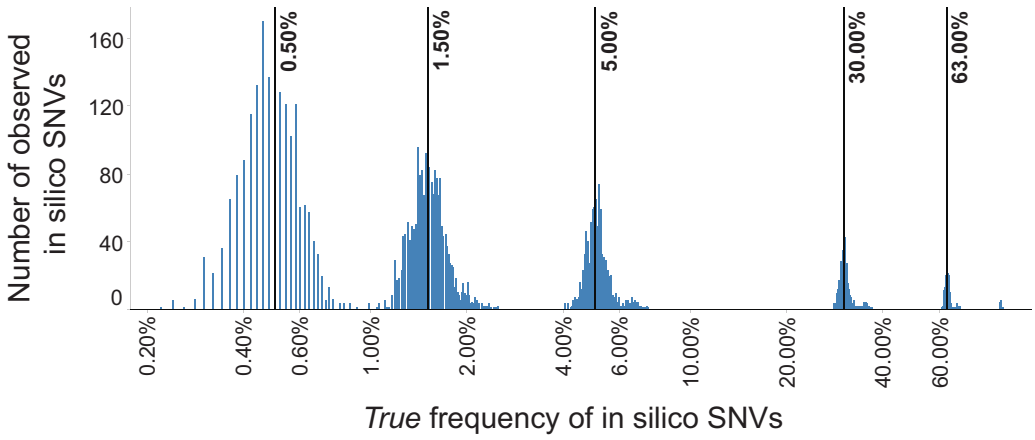

Distribution of so−called *true* frequencies of 9,600 *in silico* SNVs (10 per sample). The 1,920 variants with *true* frequency equal to 100% (always present) at position 2259 and 2927 are not shown. On the y−axis in the histogram are the number of variants with the same *true* frequency sampled around the five chosen frequencies (0.5%, 1.5%, 5%, 30%, and 63%). The *true* frequencies on the x−axis are shown in $\log_{10}$ scale.

Figure S7. QQnorm

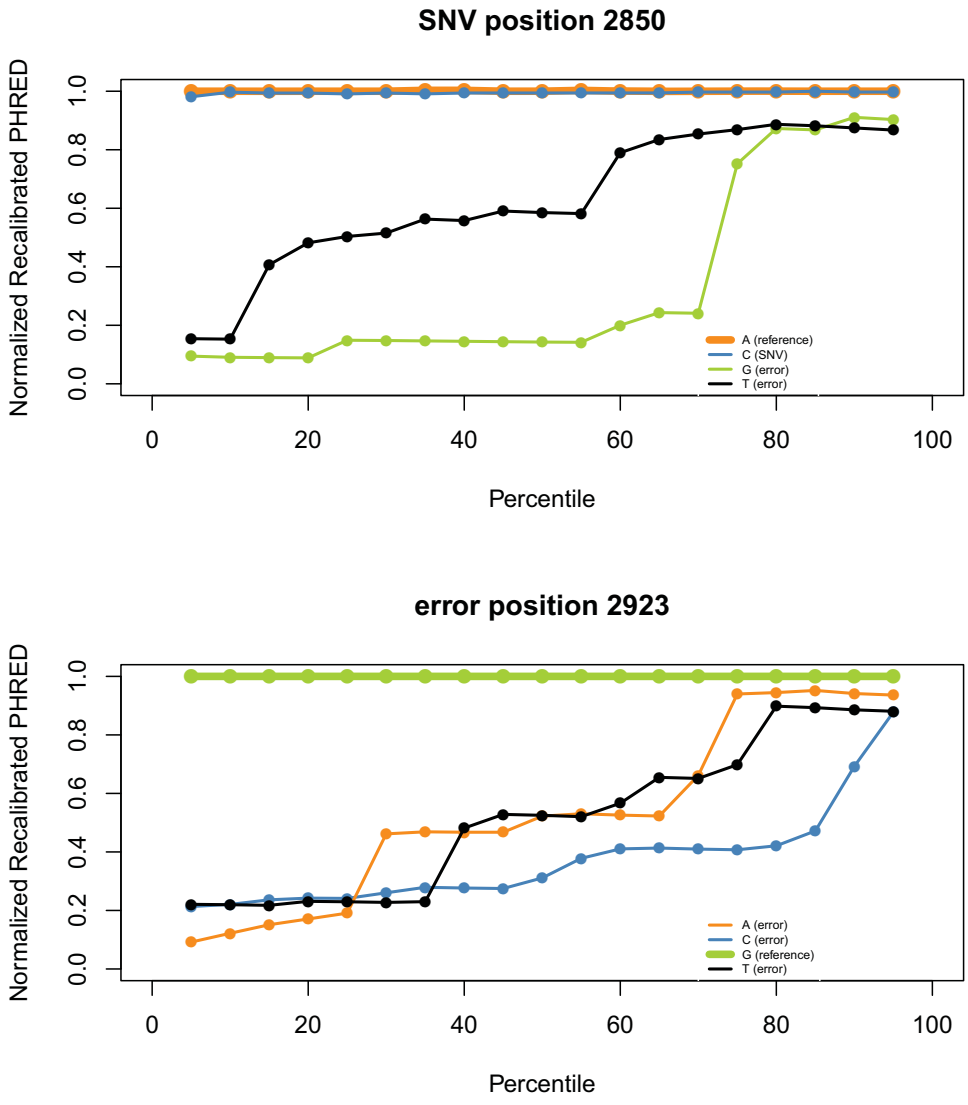

Normalized recalibrated PHRED scores per nucleotide (A/C/G/T) minimized over the read mapping direction (forward/reverse) and calculated for nineteen percentiles (5^{th},10^{th},...,95^{th}) at SNV position 2850 and at error position 2923 for training sample 1 (out of 96 *in silico* read sets).

Figure S8. QQ

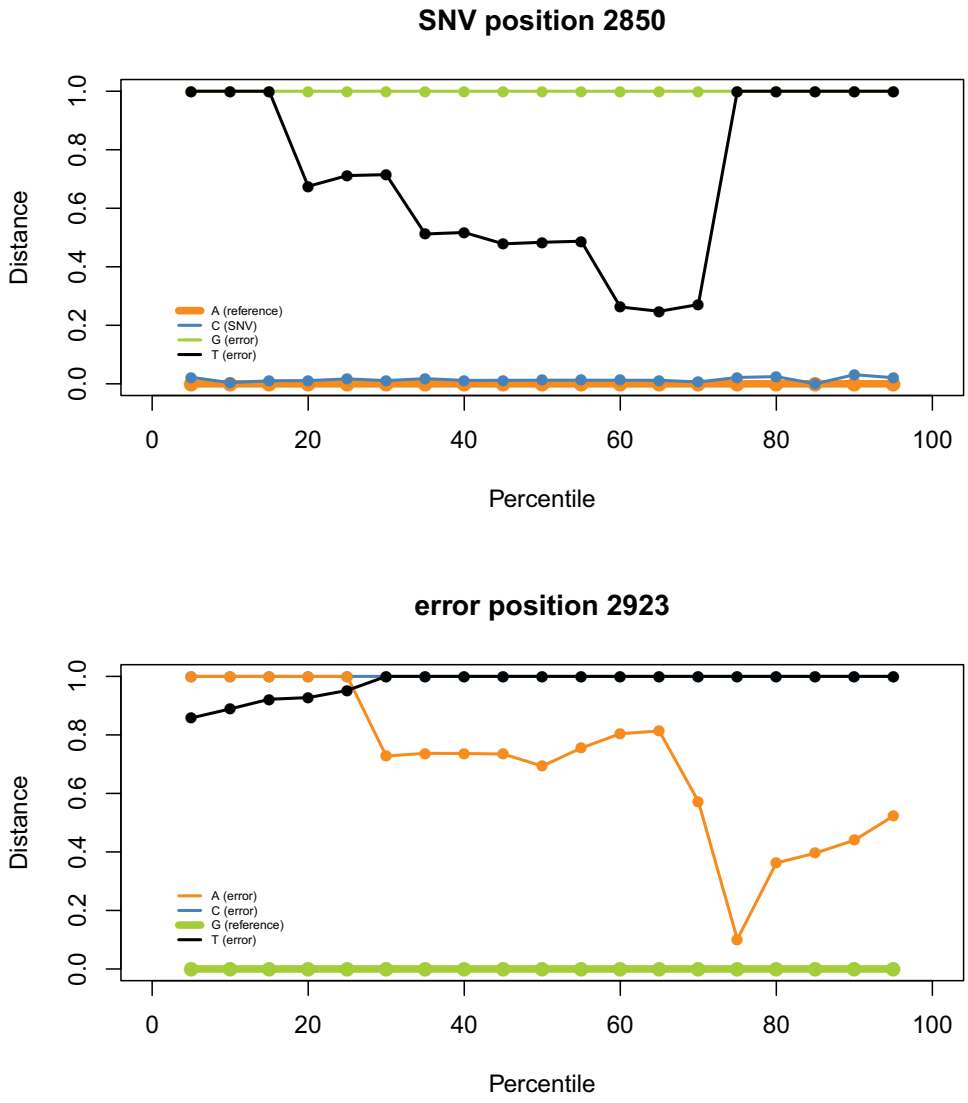

Distance per nucleotide (A/C/G/T) in the range [0,1] maximized over the read mapping direction (forward/reverse) and calculated for nineteen percentiles (5^{th},10^{th},...,95^{th}) relative to the nucleotide with worst quality at SNV position 2850 and at error position 2923 for training sample 1 (out of 96 *in silico* read sets).

Figure S9. D

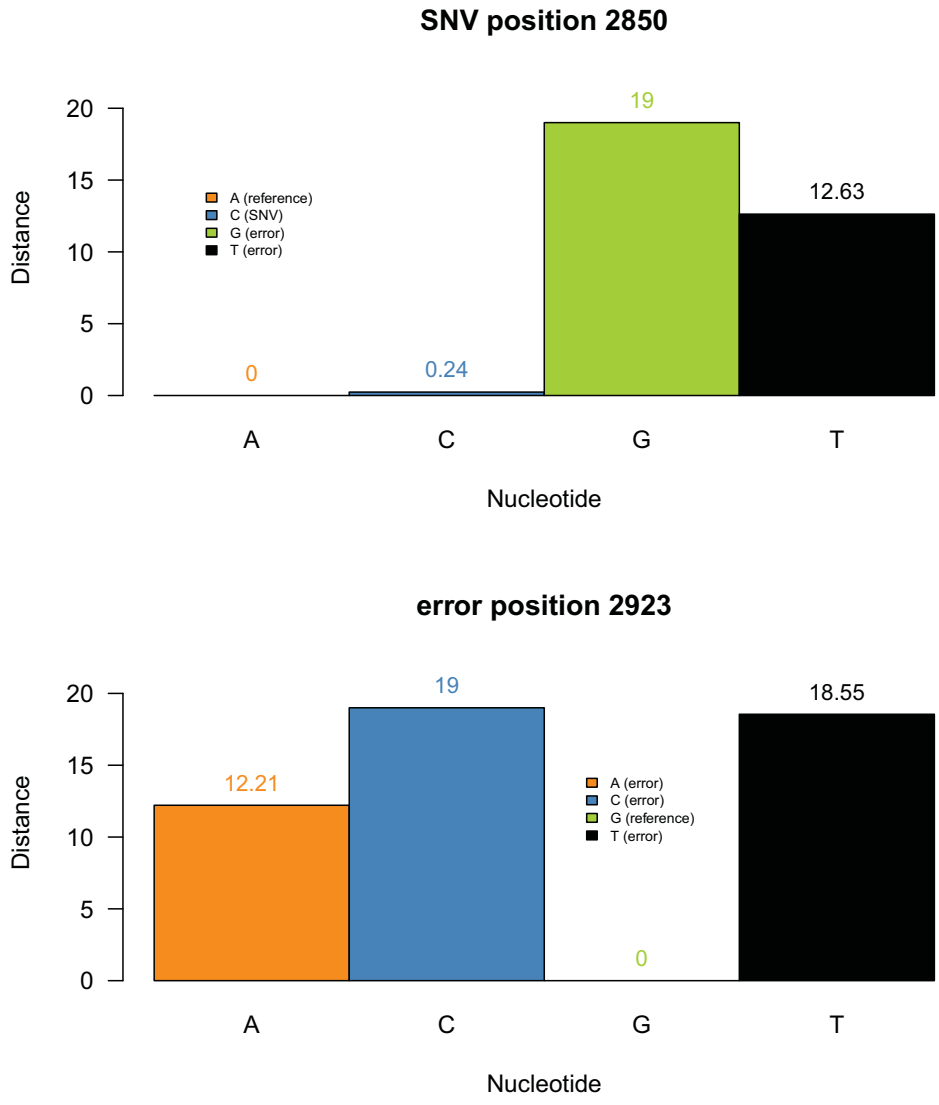

Distance per nucleotide (A/C/G/T) in the range [0,19] maximized over the read mapping direction (forward/reverse) and calculated as the sum of distances for nineteen percentiles (5^{th},10^{th},...,95^{th}) relative to the nucleotide with worst quality at SNV position 2850 and at error position 2923 for training sample 1 (out of 96 *in silico* read sets).

Figure S10.
ROC curves for QQ−SNV without variant frequency filtering on HCV plasmid mixture test datasets

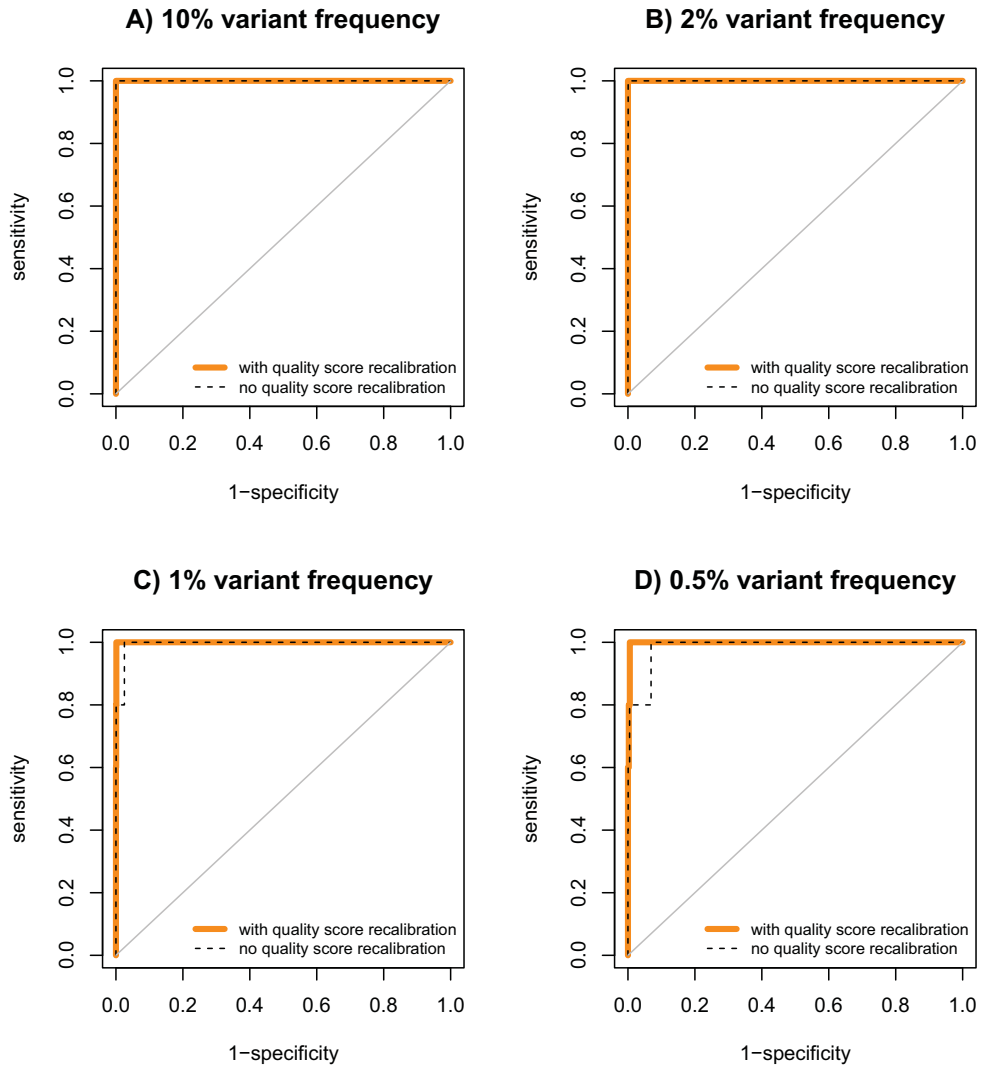

ROC curves for QQ−SNV without variant frequency filtering on HCV plasmid mixture datasets (all paired−end reads) with different spiked−in variant frequencies A) 10% B) 2% C) 1% and D) 0.5%, and comparing quality score recalibration *vs*. no quality score recalibration.

Figure S11. QQnorm.dir

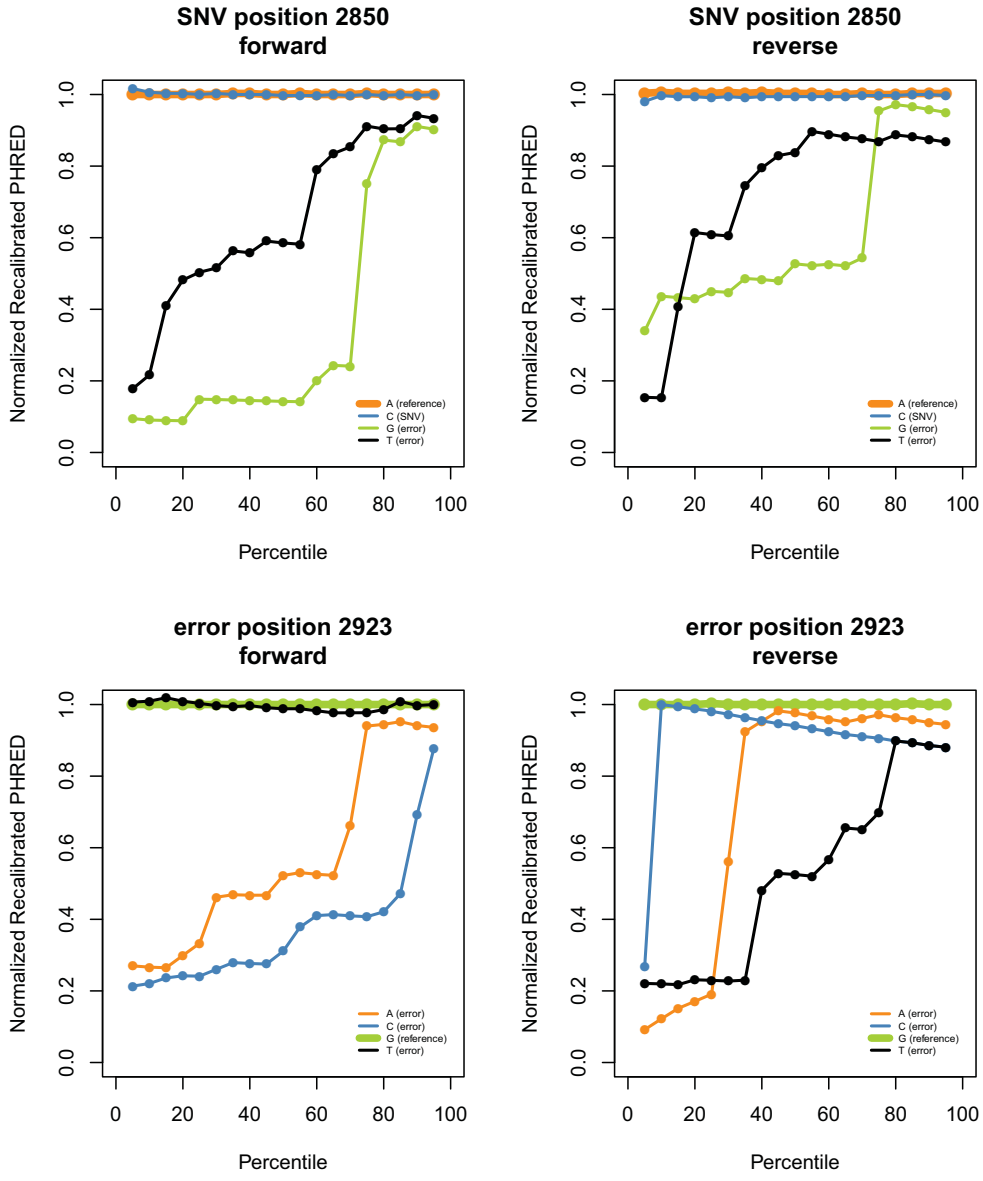

Normalized recalibrated PHRED scores per nucleotide (A/C/G/T) in the forward and reverse read mapping and calculated for nineteen percentiles (5^{th},10^{th},...,95^{th}) at SNV position 2850 and at error position 2923 for training sample 1 (out of 96 *in silico* read sets).

Figure S12. QQ.dir

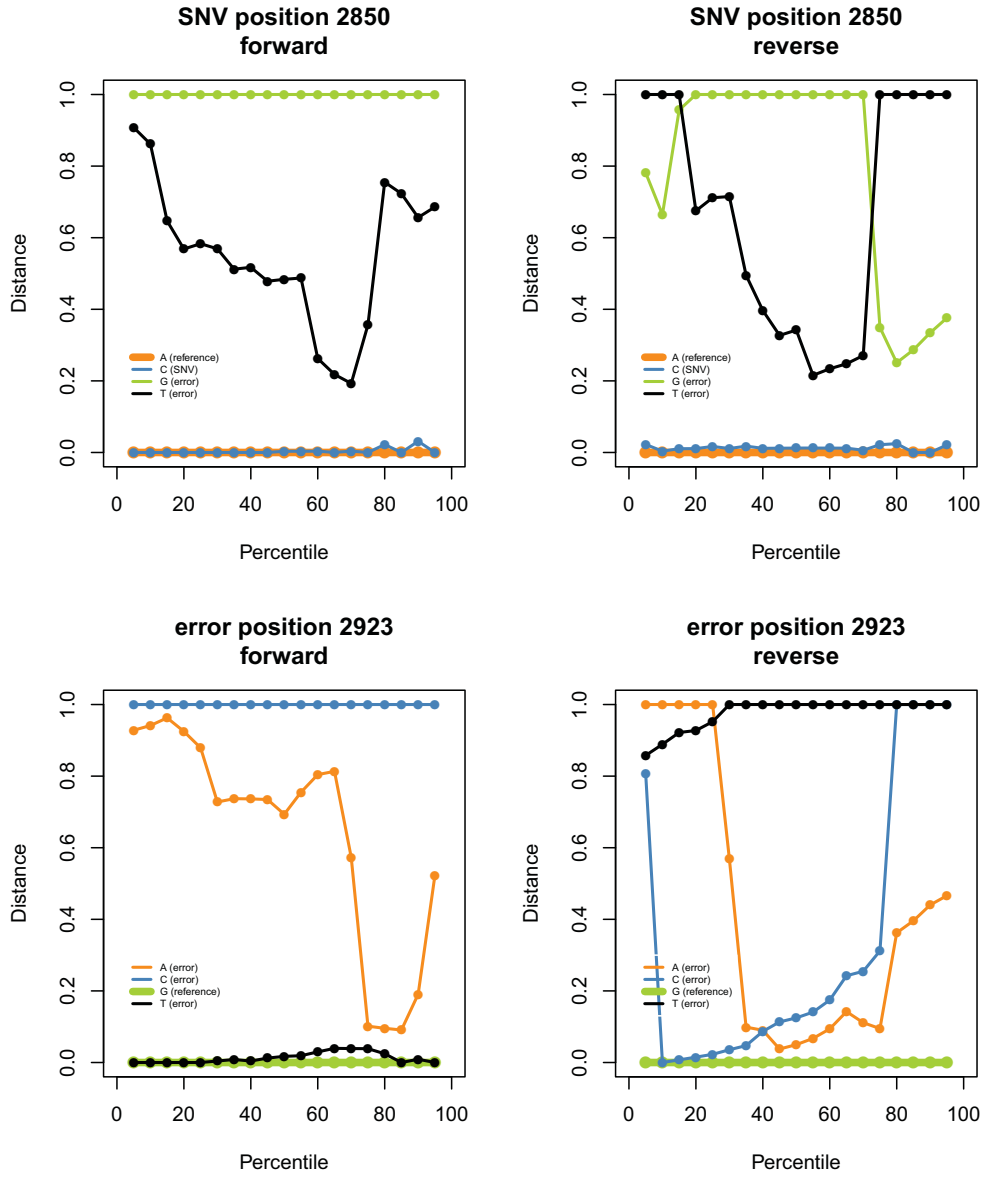

Distance per nucleotide (A/C/G/T) in the range [0,1] in the forward and reverse read mapping and calculated for nineteen percentiles (5^{th},10^{th},...,95^{th}) relative to the nucleotide with worst quality at SNV position 2850 and at error position 2923 for training sample 1 (out of 96 *in silico* read sets).

Figure S13. D.dir

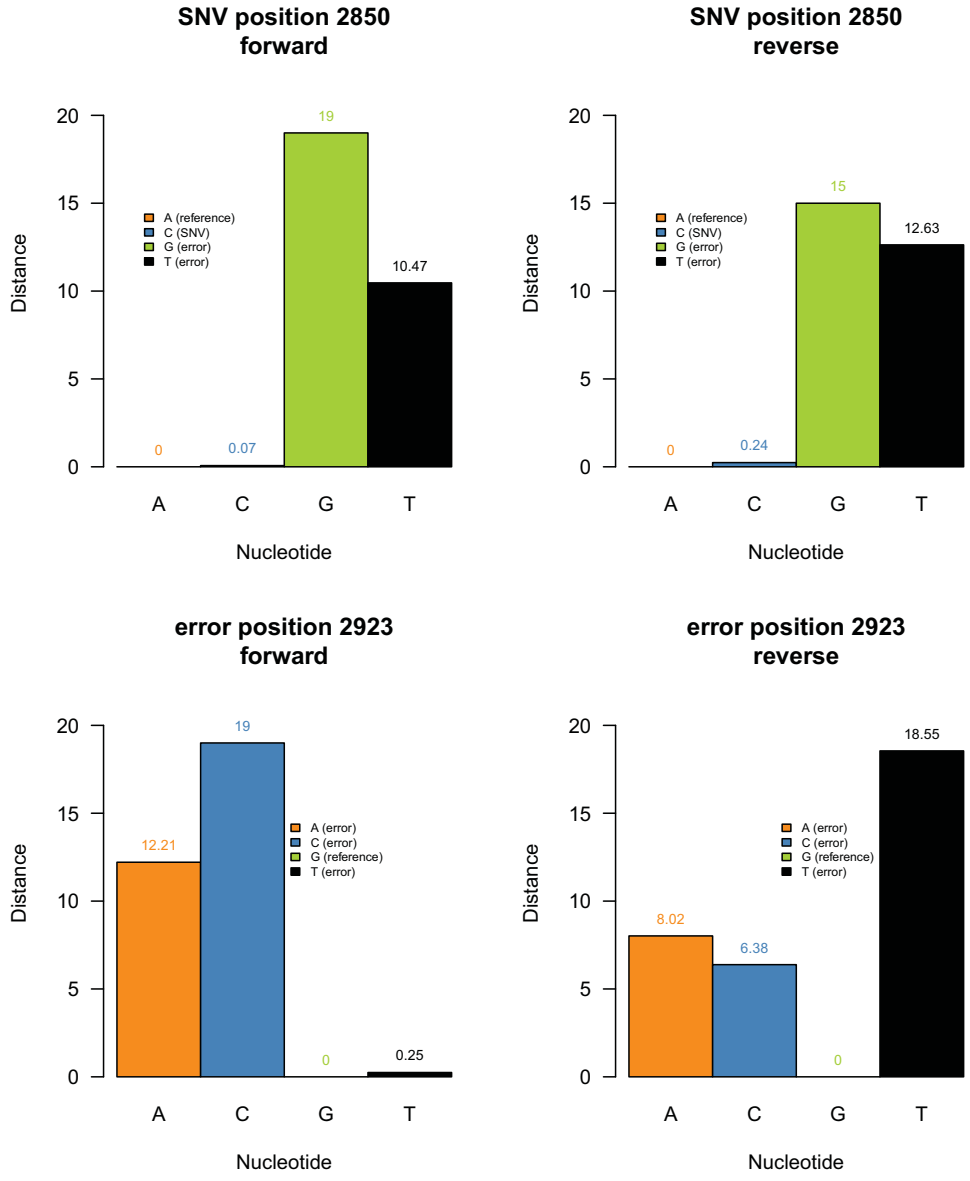

Distance per nucleotide (A/C/G/T) in the range [0,19] in the forward and reverse read mapping and calculated as the sum of distances for nineteen percentiles (5^{th},10^{th},...,95^{th}) relative to the nucleotide with worst quality at SNV position 2850 and at error position 2923 for training sample 1 (out of 96 *in silico* read sets).

Figure S14.
Training of the QQ−SNV model by weighted logistic regression

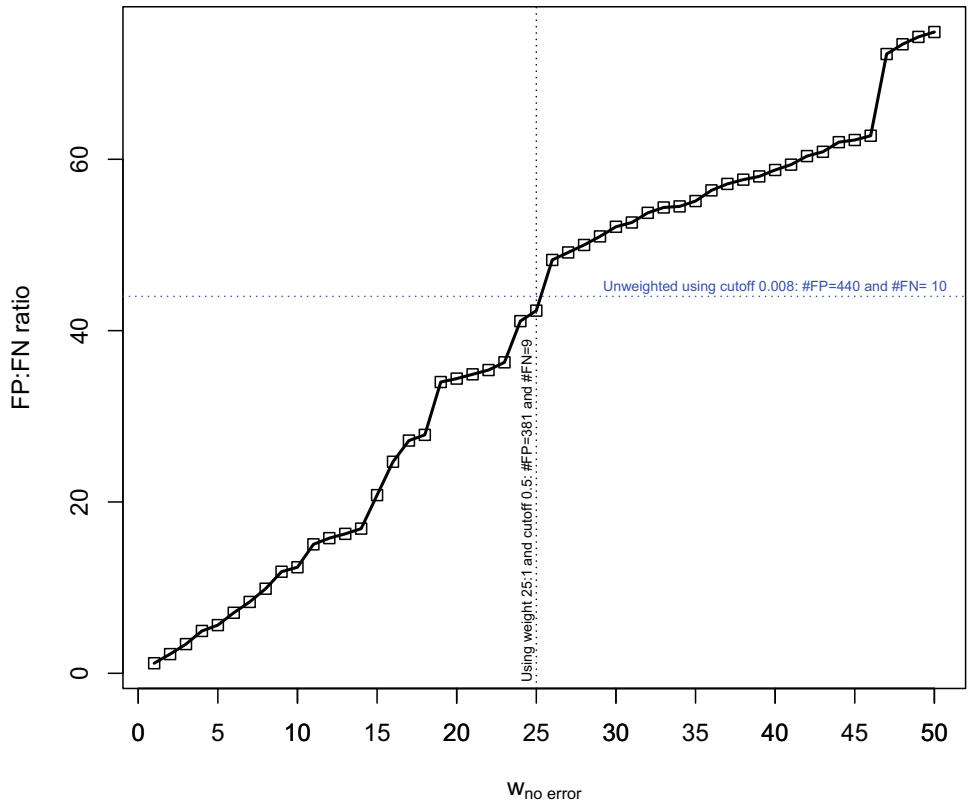

False positive : false negative ratio on the training data when varying the logistic regression weight $w_{no\ error}$ (w_{error}=1) and using cutoff 0.5 for error/no error classification (QQ−SNV_D).

Figure S15.
Performance on plasmid mixture test datasets

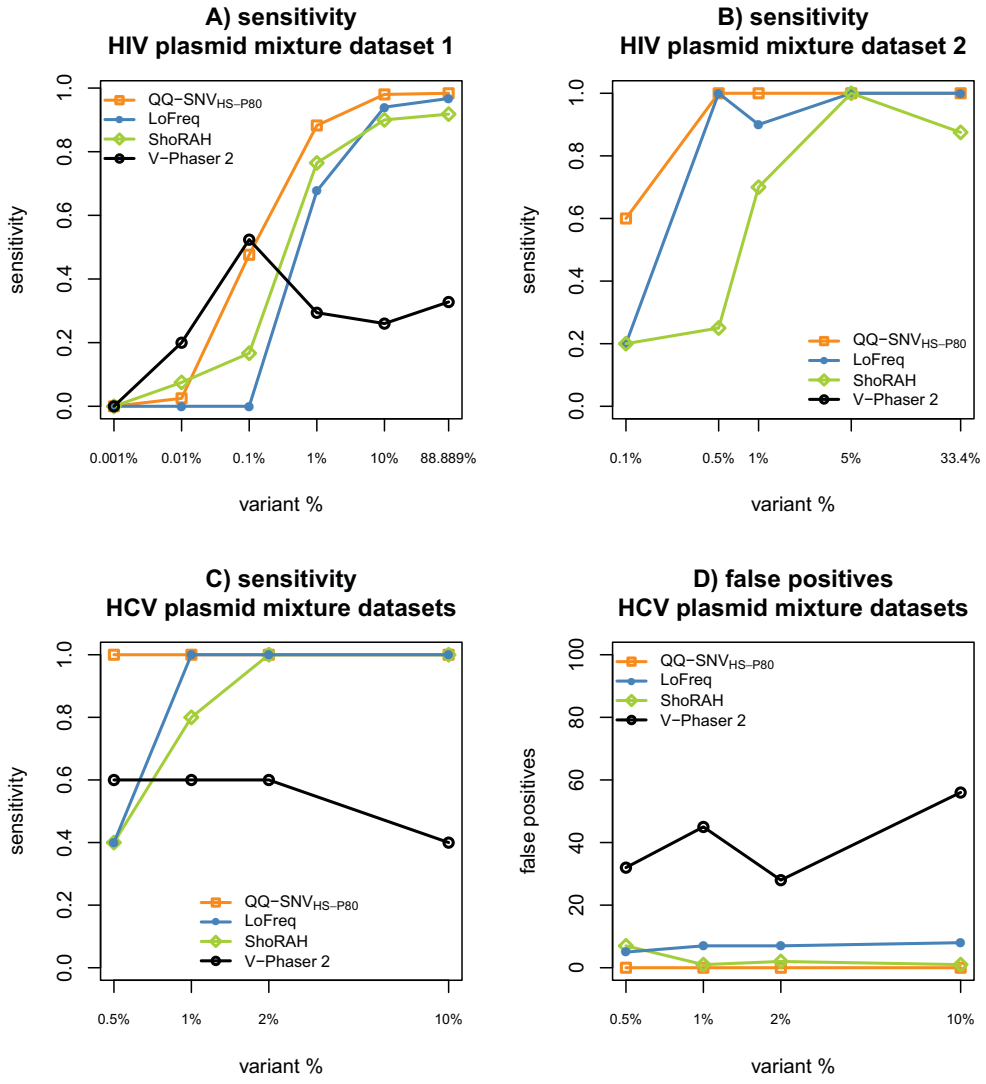

Performance of QQ−SNV$_{HS-P80}$, LoFreq, ShoRAH, and V−Phaser 2 on plasmid mixture test datasets by variant frequency (curves for Table 3−5). A) sensitivity on HIV plasmid mixture dataset 1 (Table 3). B) sensitivity on HIV plasmid mixture dataset 2 (Table 4) (variant frequencies shown for n>5 only). C) and D) sensitivity and false positives on HCV plasmid mixture datasets (all paired−end reads) (Table 5).

Figure S16.
ROC curves for QQ−SNV without variant frequency filtering at different coverage depths

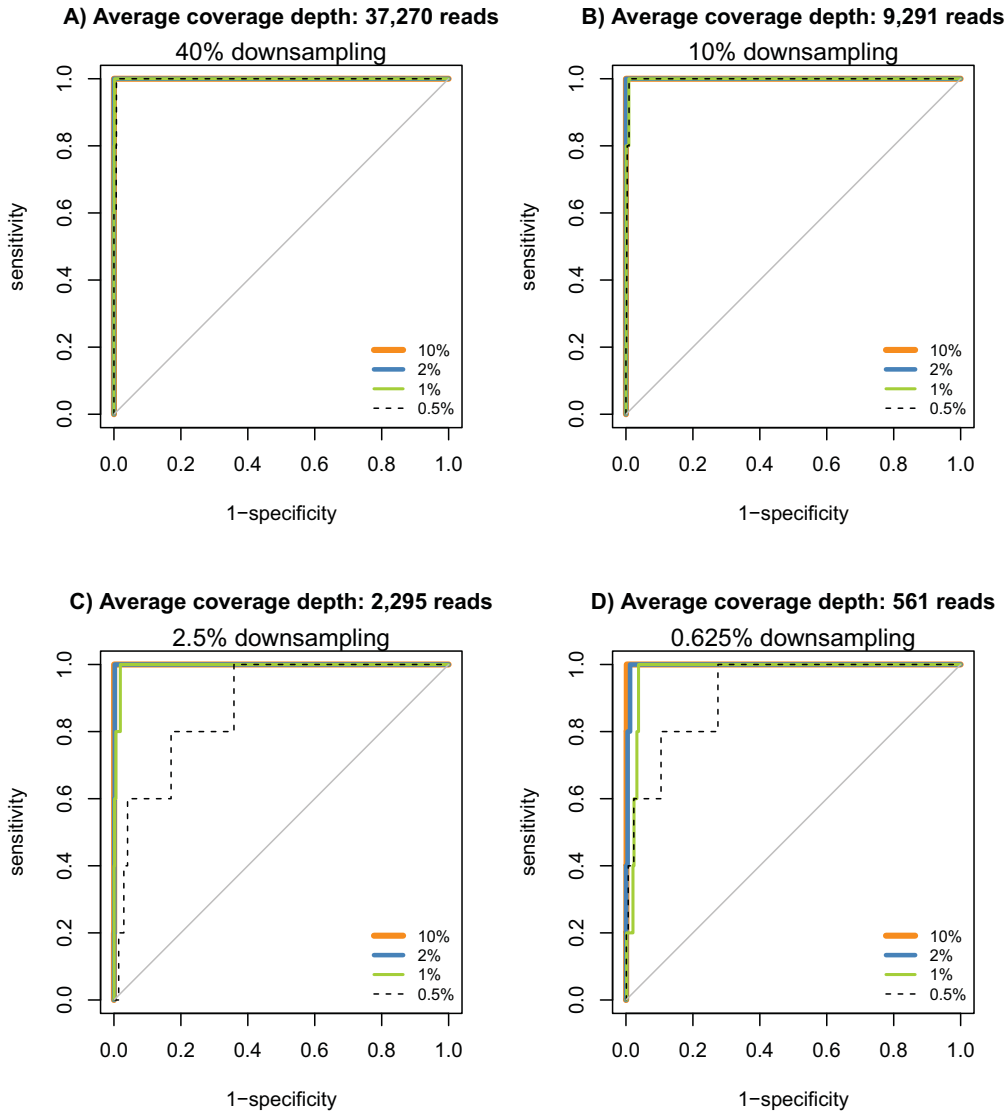

ROC curves for QQ−SNV without variant frequency filtering on HCV plasmid mixture datasets (all paired−end reads) at different coverage depths by downsampling A) 40% B) 10% C) 2.5% and D) 0.625%.

Figure S17.
ROC curves for QQ−SNV with P50 variant frequency filtering at different coverage depths

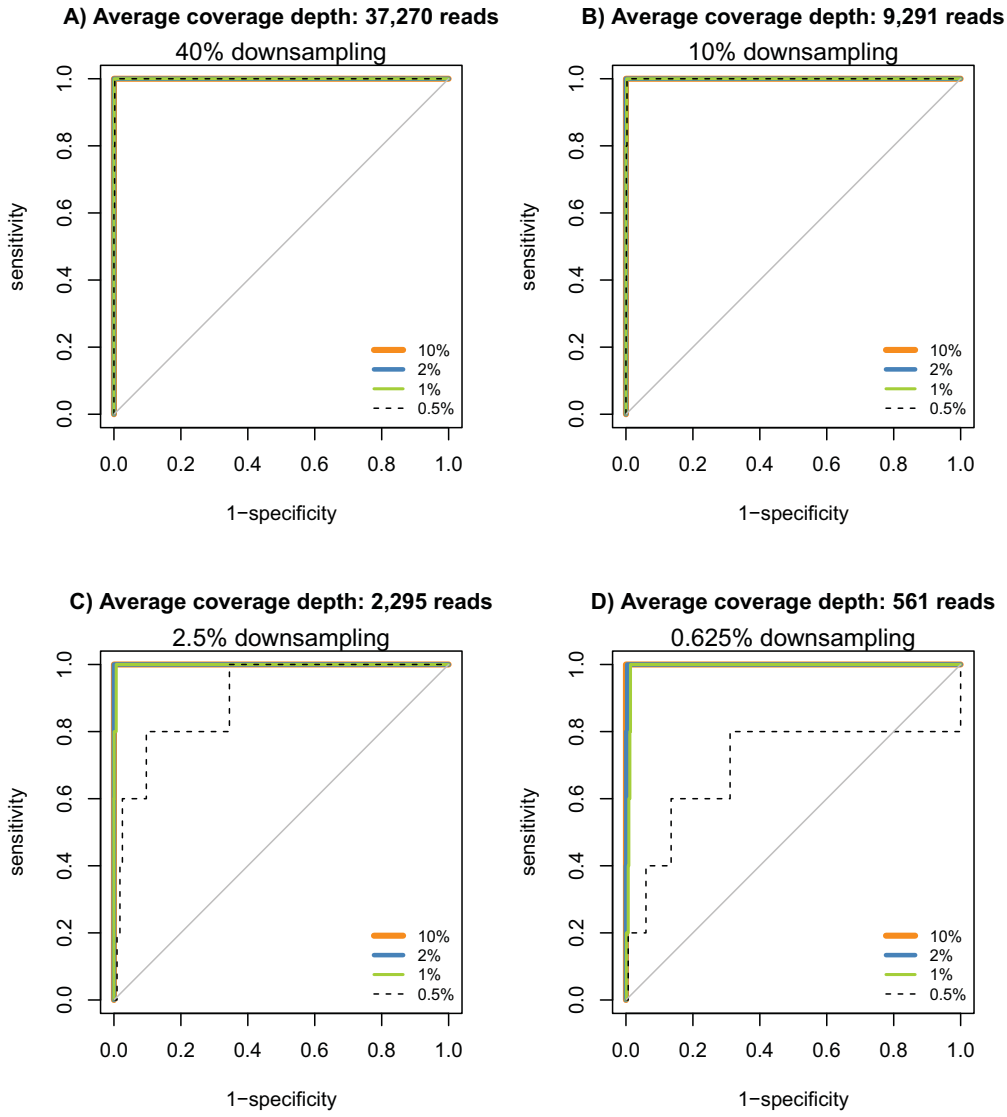

ROC curves for QQ−SNV with P50 variant frequency filtering on HCV plasmid mixture datasets (all paired−end reads) at different coverage depths by downsampling A) 40% B) 10% C) 2.5% and D) 0.625%.

Figure S18.
ROC curves for QQ−SNV with P75 variant frequency filtering at different coverage depths

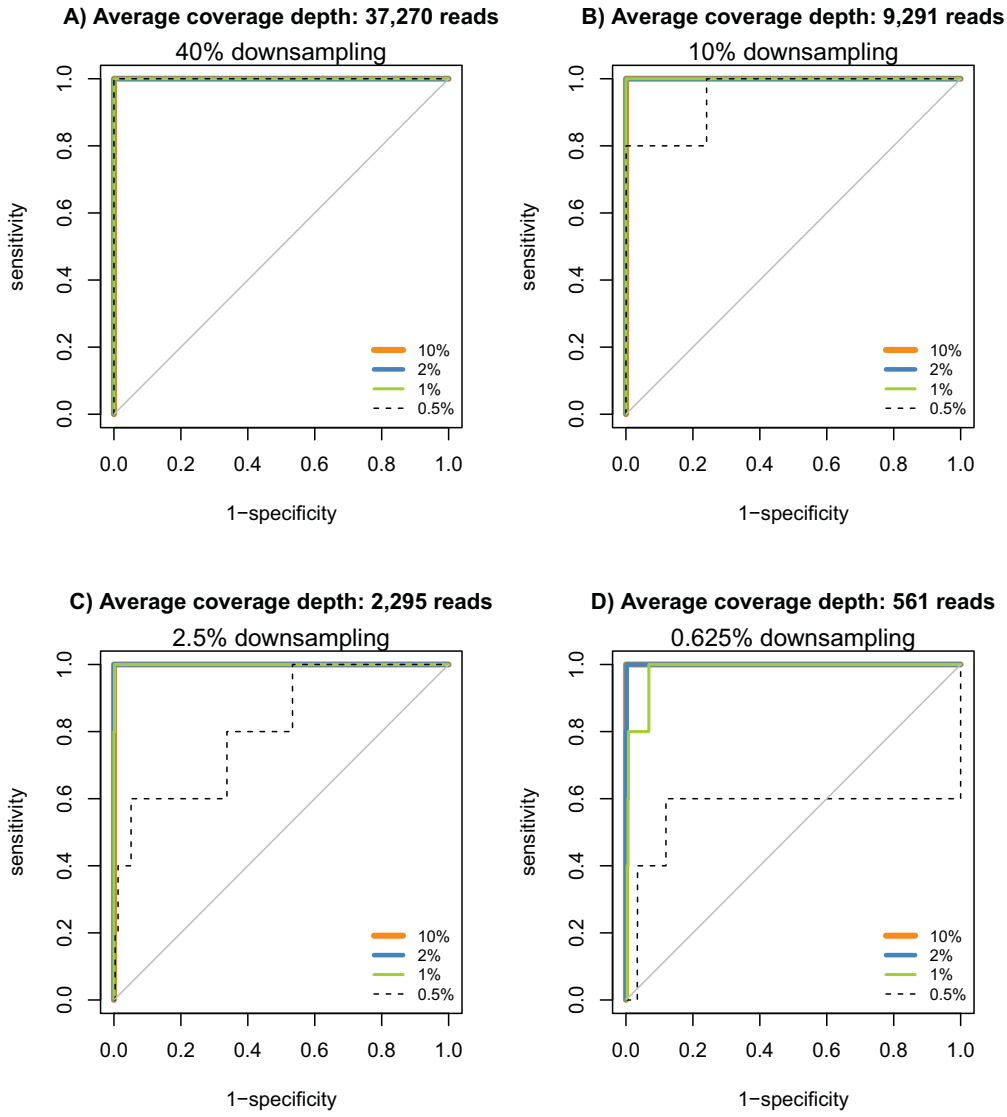

ROC curves for QQ−SNV with P75 variant frequency filtering on HCV plasmid mixture datasets (all paired−end reads) at different coverage depths by downsampling A) 40% B) 10% C) 2.5% and D) 0.625%.

Figure S19.
ROC curves for QQ−SNV with P80 variant frequency filtering at different coverage depths

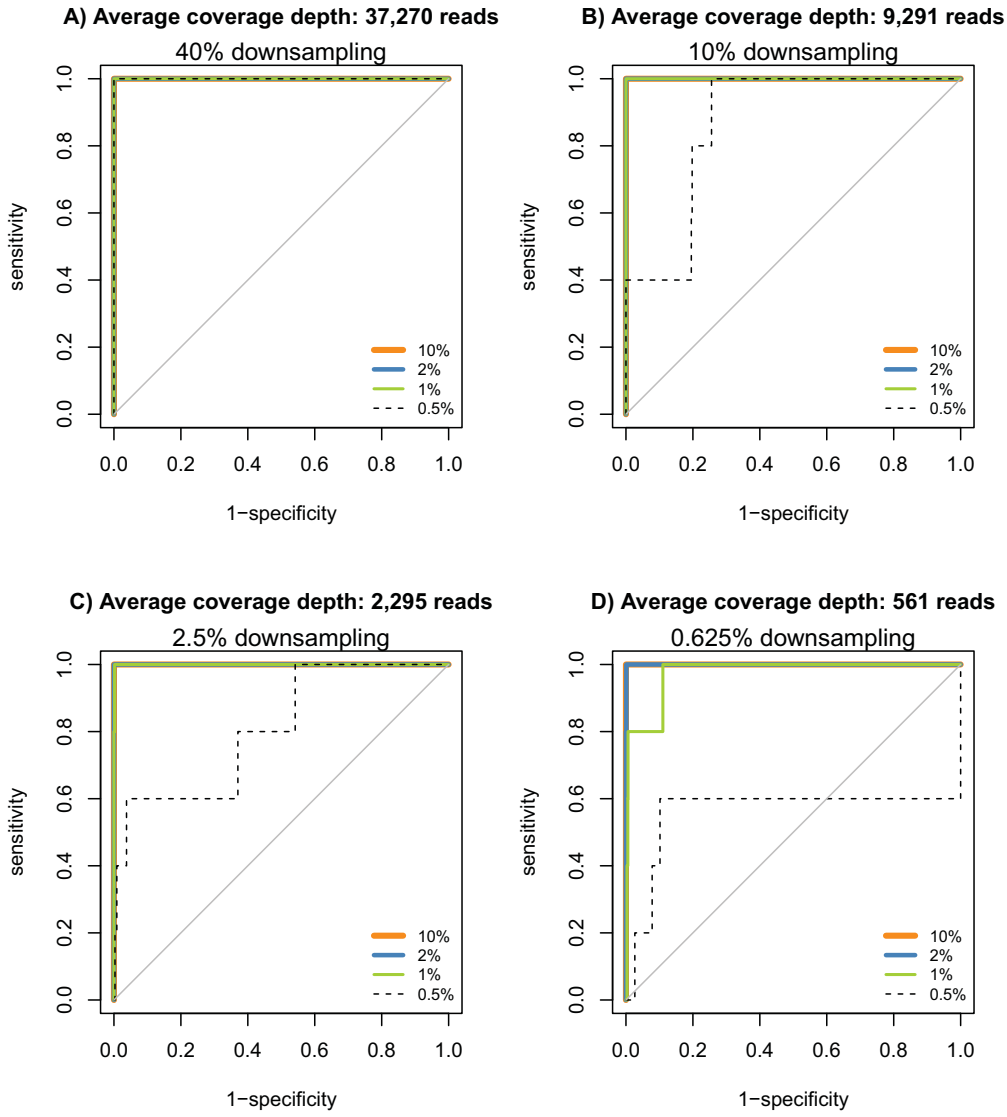

ROC curves for QQ−SNV with P80 variant frequency filtering on HCV plasmid mixture datasets (all paired−end reads) at different coverage depths by downsampling A) 40% B) 10% C) 2.5% and D) 0.625%.